Published online 4 April 2007

Nucleic Acids Research, 2007, Vol. 35, No. 10 ***3181–3191***
doi:10.1093/nar/gkm172

Determination of the DNA-binding kinetics of three related but heteroimmune bacteriophage repressors using EMSA and SPR analysis

Petri Henriksson-Peltola, Wilhelmina Sehlén and Elisabeth Haggård-Ljungquist*

Department of Genetics, Microbiology and Toxicology, Stockholm University, S-106 91 Stockholm, Sweden

Received August 11, 2006; Revised March 5, 2007; Accepted March 6, 2007

ABSTRACT

Bacteriophages P2, P2 Hy *dis* and WΦ are very similar but heteroimmune *Escherichia coli* phages. The structural genes show over 96% identity, but the repressors show between 43 and 63% identities. Furthermore, the operators, which contain two directly repeated sequences, vary in sequence, length, location relative to the promoter and spacing between the direct repeats. We have compared the *in vivo* effects of the wild type and mutated operators on gene expression with the complexes formed between the repressors and their wild type or mutated operators using electrophoretic mobility shift assay (EMSA), and real-time kinetics of the protein–DNA interactions using surface plasmon resonance (SPR) analysis. Using EMSA, the repressors formed different protein–DNA complexes, and only WΦ was significantly affected by point mutations. However, SPR analysis showed a reduced association rate constant and an increased dissociation rate constant for P2 and WΦ operator mutants. The association rate constants of P2 Hy *dis* was too fast to be determined. The P2 Hy *dis* dissociation response curves were shown to be triphasic, while both P2 and WΦ C were biphasic. Thus, the kinetics of complex formation and the nature of the complexes formed differ extensively between these very closely related phages.

INTRODUCTION

The immunity repressors of the temperate P2-like phages can be divided into two types depending on size, sequence similarity and control; the 186-like CI proteins and the P2-like C proteins (1). The P2-like C proteins are small homologous proteins of ~100 aa. They recognize two direct repeats and are expressed from one promoter only. The C proteins of phage P2, P2 Hy *dis* and Wϕ represent three different immunity classes, and so far the only C proteins where the operators have been located (2–4). The identity between the immunity C repressors is 38% (P2/P2Hy *dis* 63%, P2/Wϕ 43% and Wϕ/P2 Hy *dis* 44% identity at the amino acid level) (Figure 1A). The C proteins recognize direct repeats, termed half-sites, but the repeats differ in sequence, lengths, locations relative to the early promoters, and spacing (Figure 1B). P2 C binds to two direct repeats of 8 bp with a center-to-center distance of 22 bp. In P2 Hy *dis*, the half-sites are 8 bp with a distance of 26 bp, and the half-sites of Wϕ are 10 bp long with a distance of 34 bp. In P2 and Wϕ, the operators are flanking the −10 region of the Pe-promoter compared with P2 Hy *dis* where the half-sites are located on either side of the –35 region of the Pe-promoter.

To compare the affinities and the binding capacities of P2 C, P2 Hy *dis* C and Wϕ C to their wild type and mutated operators, we have used one *in vivo* and two *in vitro* methods. To analyze the effects of the respective C protein on Pe *in vivo*, a plasmid system has been used where a reporter gene is under the control of the respective Pe promoter/operator region and the C protein is supplied in *cis*. Electrophoretic mobility shift assays (EMSA) have been used to analyze the complexes formed by the repressors with their respective operator and their dissociation constants. To determine the kinetics of the repressor–operator interactions in real time, we have used surface plasmon resonance (SPR) analysis.

MATERIALS AND METHODS

Biological materials

Bacterial strains and plasmids used are shown in Table 1.

Chloramphenicol acetyltransferease (CAT) activity determination

Ten milliliter cultures were harvested at an OD_{600} of 0.8. The cultures were washed in 100 mM Tris–HCl, pH 7.9 and lyzed by sonication in a total volume of 2 ml, and the cell extracts were cleared by centrifugation. Total protein

*To whom correspondence should be addressed. Tel: +46 8 161270; Fax: +46 8 164315; Email: Elisabeth.Haggard@gmt.su.se

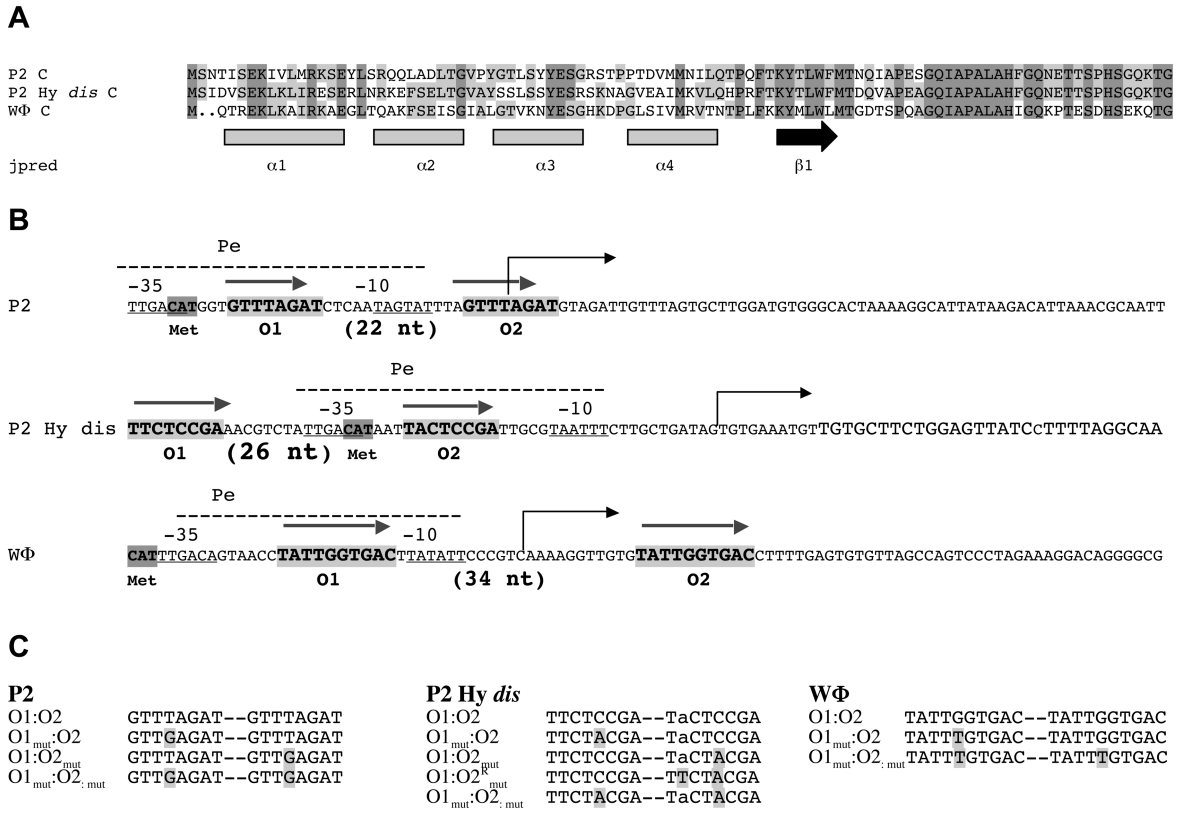

Figure 1. A comparison of the amino acid sequences of the C proteins and organization of the promoter–operator regions of P2, P2 Hy *dis* and Wϕ. (**A**) The amino acid sequence of the C proteins and the predicted secondary structure. Amino acids conserved among all three proteins are shaded in dark gray; amino acids conserved among two proteins are shaded in light gray. (**B**) DNA sequences of the early promoter–operators of P2, P2 Hy *dis* and Wϕ. The locations of the −10 and −35 regions are underlined. The transcriptional start sites are indicated by bent arrows. The operator half-sites are shaded in light gray, and the initiation codons are shaded in dark gray. The center-to-center distances between the half-sites are indicated in parenthesis. (**C**) The DNA sequences of the wt and mutated operators used in this work. The mutated nucleotide are shaded in gray.

Table 1. Bacterial strains and plasmids used

Strain or plasmid	Pertinent features	Origin/reference
Escherichia coli strains		
BL21(DE3)	*omp*T *hsd*R *hsd*M *lon E. coli* B strain with T7 RNA polymerase under control of *lac* promoter	5
Plasmids		
pEE675	pKK232-8 derivative with P2 Pe-Pc region where Pe directs the *cat* gene	6
pEE679	pET8c derivate with P2 *C* gene under the control of the T7 promoter. This plasmid has been found to contain a tandem DNA fragment downstream of the *C* gene from phage P4 (7870–8582)	7
pEE905	pKK232-8 derivative with Wϕ Pe-Pc region where Pe directs the *cat* gene	3
pEE909	pEE905 derivative with 1 mutation in O1 site	3
pEE911	pEE905 derivative with 1 mutation in both O1 and O2 sites	3
pEE915	pKK232-8 derivative with P2 Hy *dis* C-Pe-Pc region where Pe directs the *cat* gene	4
pEE916	pEE915 derivative with 1 mutation in O1 site	4
pEE917	pEE915 derivative with 1 mutation in O2 site	4
pEE918	pEE915 derivative with 1 mutation in both O1 and O2 sites	4
pEE922	pET8c derivative with P2 Hy *dis C* gene under the control of the T7 promoter	4
pEE1020	pET8c derivative with Wϕ *C* gene under the control of the T7 promoter	8
pEE1021	pEE675 derivative with 1 mutation in O1 site	Renberg-Eriksson[a]
pEE1022	pEE675 derivative with 1 mutation in O2 site	Renberg-Eriksson[a]
pEE1023	pEE675 derivative with 1 mutation in both O1 and O2 sites	Renberg-Eriksson[a]
pET8c	pBR322 derivative containing T7 promoter	5
pKK232-8	pBR322 derivative containing a promoterless *cat* gene	9
pLysS	Plasmid expressing low level of T7 lysozome	5

[a]Unpublished

concentration was determined by the Bradford method using bovine serum albumin as standard (10). The supernatants were diluted and an equal amount of protein was added for the CAT determinations with [^{14}C]-chloramphenicol. The acetylated forms were separated by thin-layer chromatography (11). The CAT activity was determined after phosphor image analysis (Fuji Film FLA-3000) as the amount of acetylated chloramphenicol divided by the total amount of chloramphenicol.

Protein purification

Escherichia coli strain BL21(DE3) (5) containing plasmids pEE679 expressing P2 C (6), pEE922 expressing P2 Hy *dis* C (4), or pEE1020 expressing Wϕ C (8), were grown at 37°C in LB or M9 minimal medium with ampicillin (100 μg/ml). The proteins were overexpressed and purified as described previously (8). The protein concentrations were determined by the Bradford method (10).

The purified proteins were stored in 10 mM sodium phosphate pH 7.0 supplemented 0.4 M NaCl for P2 C and P2 Hy *dis* C, and 0.6 M NaCl for Wϕ C, at 4°C either with 40% (v/v) glycerol for EMSA or without glycerol for SPR analysis.

Electrophoretic mobility shift assay (EMSA)

The DNA fragments containing the wild-type operators (O1:O2), operators with a point mutation in one of the half-sites (O1mut : O2) or operators with a point mutation in both half-sites (O1mut: O2mut) (Figure 1), were amplified using primers 7 + 28R (GCATTAAGACTATCTTCTCG) and pKK240L (CCTTAGCTCCTGAAAATCTCG) with plasmid pEE675, pEE1021 or pEE1023 as sub-strates for the P2 operators, primers Wϕ 8R (GCTTTCCTAA TCGCTTTCAG) and pKK232HindII (GTCCTACTC AAGCTTGGCTG) with plasmids pEE905, pEE909 or pEE911 as substrates for the Wϕ operators and primers A3-44 (CCTTTCAGATTCACGG) and pKK240L (CCTT AGCTCCTGAAAATCTCG) with plasmids pEE915, pEE916 or pEE918 for the P2 Hy *dis* operators. The lengths of the PCR fragments containing the operators were for P2 233 nt, for Wϕ 259 nt and for P2 Hy *dis* 228 nt. Also, 100 ng of the templates were 5′ end labeled with T4 polynucleotide kinase (Fermentas, Hanover, MD, USA) and [γ-^{32}P]-ATP (GE Healthcare, Piscataway, PA, USA). The labeled fragments were purified from the unincorporated nucleotides using MicroSpin G-25 columns (GE Healthcare) and after the purification the final DNA concentration assuming 100% recovery would be 22 nM in the stock solution. The labeled and purified DNA was incubated for 30′ at 30°C with different amounts of the protein in a BB buffer containing 12 mM HEPES, 12% glycerol, 4 mM Tris–HCl pH 7.9, 60 mM KCl, 1 mM EDTA, 1 mM DTT, 0.001 μg/μl dI/dC and 0.06 μg/μl BSA in a volume of 25 μl, where the final DNA concentration was 1 nM. The samples were loaded onto the 5% non-denaturating polyacrylamide gel immediately after incubation. The protein concentrations used are stated in the figure legends. The C protein was kept in 10 mM sodiumphosphate pH 7.0 with 0.4 M NaCl for P2 C and P2 Hy *dis* C and 0.6 M NaCl for Wϕ C. The protein was diluted in the same buffer. The gels were vacuum dried before the phosphor imager analysis.

The DNA fragments containing the wild-type operator (O1:O2) of each phage, as described above, were used to determine the dissociation constants (K_D) of each C repressor. The labeled and purified DNA was incubated with increasing concentrations of the protein in a BB buffer, as above, and the final DNA concentration in each reaction was 1 nM. The samples containing different concentrations of protein but the same amount DNA were loaded into the 5% non-denaturating PAA. The gel was vacuum dried. The separated radioactivity was analyzed and quantified using the phosphor imager (Fuji Film FLA-3000). Dissociation constants were determined after fitting the 1:1 binding isotherm to the experimental data by using the SIMFIT program (url:http// www.simfit.man.ac.uk).

Real-time kinetic analyses

Surface plasmon resonance analyses were carried out using the Biacore 3000 system (Biacore, Uppsala, Sweden). The operator containing DNA fragments described in the EMSA above were amplified by PCR using the phage specific primers and the biotinylated vector primer, biopKK232HindII (GTCCTACTCAAGC TTGGCTG) that had a biotin molecule attached to its 5′ end. A sensor chip (SA) (Biacore) containing a streptavidin surface was activated by three consecutive injections of 1 M NaCl + 50 mM NaOH. Approximately 0.5 ng of the different operator fragments were immobilized in the respective flow cell, which corresponds to 200–300 RU for P2 C and P2 Hy *dis* C and for Wϕ C 300–344 RU. The HBS-EP buffer (0.01 M HEPES, pH 7.4, 0.15 M NaCl, 3 mM EDTA, 0.005% Surfactant P20) was used as an immobilization buffer (Biacore). The proteins were diluted in the running buffer, which was the same as the immobilizing buffer. The protein concentrations used are given in the text. Two different flow rates were used, 30 and 2 μl/min and two injection cycles were performed. After each cycle, the chip was regenerated by washing with consecutive injections of 1 M NaCl and 50 mM NaOH. The SPR data was evaluated using the BIAevaluation software from (Biacore). Since the response curves were di- or triphasic the k_a and k_d-values were determined separately for specified parts of the sensorgrams, and the fastest k_a and the slowest k_d-values were used for the K_A and K_D determinations.

RESULTS

Different operator constructs have been used for each phage. The wild type or mutated operators were used to determine the affinity and the binding capacity of the respective C repressor. Two of the mutated operators contained one point mutation in either O1 or O2 and in the third both half-sites were mutated (Figure 1). The purpose of mutating the operators was to investigate how the mutations affect the affinity and the binding strength between the C repressor protein and the operator for a comparison of their *in vivo* effects.

The capacities of the C proteins to repress their cognate promoter *in vivo* using wild type and mutated operators and a plasmid reporter gene system

The effects of the operator mutants used in this work have been analyzed for Wϕ C, using the *cat* gene as a reporter (3). Mutations in just one operator half-site did not affect the capacity of the C protein to repress the reporter gene, but when both half-sites were mutated the CAT activity was as high as the fully derepressed Pe promoter.

To investigate the *in vivo* effects of the operator mutations of P2 and P2 Hy *dis*, the C-Pe-Pc region of each phage was cloned upstream of the promoterless *cat* gene of plasmid pKK232-8 (9), and the capacity of the respective C protein to repress Pe was determined by measuring the CAT activity.

The mutation in either O1 or O2 half-site of the P2 operator does not abolish the repression capacity since the CAT-activity is as low as with the wild-type operator (Figure 2A, lanes 2, 3 and 5). However, mutations in both half-sites reduce the capacity of the P2 C protein to repress Pe since the CAT activity was 24% of the fully derepressed P2 promoter, i.e., in the absence of the C protein (Figure 2A, lanes 1, 4).

Since the operator of P2 Hy *dis* contains a natural mutation in O2 (4) (Figure 1), the repression pattern differs between P2 or Wϕ Pe as seen in Figure 2B. The point mutation in O1 has no affect on the repression capacity, since the CAT activity is as low as with the wild-type operator (lanes 2 and 3), but when a point mutation is introduced in O2, the repression of the *cat* gene is abolished since the CAT activity is as high as the fully derepressed Wϕ Pe promoter and operator with a mutation in both half-sites (lanes 1, 5 and 6). A correction of the natural mutation in combination with the O2 mutation (O^{R}_{mut}) gives a full repression of the *cat* gene (lane 4).

The P2, P2 Hy dis and Wϕ C proteins give different band patterns in electromobility shift analysis

At the N-terminus of the repressors there are three alpha helices, and the 2nd and 3rd helix may constitute a HTH motif where the 3rd helix would be the DNA recognition helix. This assumption is supported by the fact that the C proteins differ in the 3rd helix (Figure 1A), but the 3D structure has not yet been determined. In contrast to most phage repressors the P2 C protein recognizes two direct repeats. It has been shown to form dimers, and the dimerization domain has been located to the C-terminal part of the protein (6,12).

The band shifts generated with P2 C are shown in Figure 3A. The P2 C protein gives two major band shifts, I and II (lanes 2–5). This fits with previous observations using crude extracts (6). The point mutations in O1 (lanes 7–10) or in both O1 and O2 (lanes 12–14) have no large effects on the band pattern. It should be noted that the single point mutations in O1 or O2 do not affect the capacity of C to repress the Pe promoter, while the double O1 and O2 mutation will reduce the capacity of C to repress Pe *in vivo* (Figure 2A).

The band pattern generated with P2 Hy *dis* C and its operator is similar to what has been observed using crude extracts (Figure 3B, lanes 2–5) (4). The major complex formed (II) has a very slow mobility compared to complex II formed by P2 C binding to its operator. A point mutation in O2 (lanes 6–10) or in both O1 and O2 (lanes 12–15) has no major effects on the complexes formed. *In vivo* it has been shown that the O2 mutation is enough to make Pe refractory to repression by P2 Hy *dis* C (4). Thus, the band pattern does not reflect the capacity of the C protein to repress the Pe promoter. The differences in migration of the protein–DNA complexes formed with P2 and P2 Hy *dis* proteins can either be due to different number of C proteins bound per operator or that the proteins cause different conformations of the DNA target.

Wϕ C shows three retarded bands with the wild-type operator, I, II and III (Figure 3C, lanes 2–5). Complex III has about the same mobility as complex II obtained with P2 C (Figure 3A). A point mutation in O1 leads to a loss of the weak band I (lanes 7–10), and having a point mutation in both O1 and O2, which *in vivo* makes the Wϕ C protein unable to repress expression of the *cat* reporter gene, gives the strong retarded band I, no band II and a relative decrease of radioactivity in band III (lanes 12–15). The decrease in the formation of complex III only when both half-sites are mutated, is in agreement with the *in vivo* data where the single point mutation does not affect the capacity of Wϕ C to block the Pe promoter while the double mutant is refractory to the presence of Wϕ C (2).

Estimation of the dissociation constants (K_D) of the C repressor/DNA complexes from electromobility shift analysis

Since the complexes formed between the C proteins and the respective operator varied, we were interested to determine their dissociation constants, using EMSA. Thus, a titration with a constant amount of DNA and an increasing amount of C protein was performed for each repressor-operator system, and the percent shifted DNA for each C repressor was quantified and analyzed by plotting the amount of shifted DNA against the protein concentrations (Figure 4A–C). The least-squares fit was used to generate the curves, and transformed for a linear regression analysis $[DNA]_{free}/[complex] = K_D \times 1/[protein]_{total}$ (data not shown) (13). Since the specific activity of different C protein preparations varied, the K_D-values have been calculated from the preparations having the highest specific activities, which in the case of P2 Hy *dis* C corresponds to that used in Figure 3. The K_D for P2 C was estimated to 2.4×10^{-10} M, for P2 Hy *dis* C to 3.5×10^{-9} M and for Wϕ C to 2.2×10^{-9} M (Figure 4).

An analysis of the interactions between the respective C protein with their wild type and mutated operators using surface plasmon resonance (SPR)

The determination of K_D-values using EMSA is dependent on the specific activity of the purified protein. Since the specific activity of our C preparations varied, we were interested to compare the values obtained by EMSA with

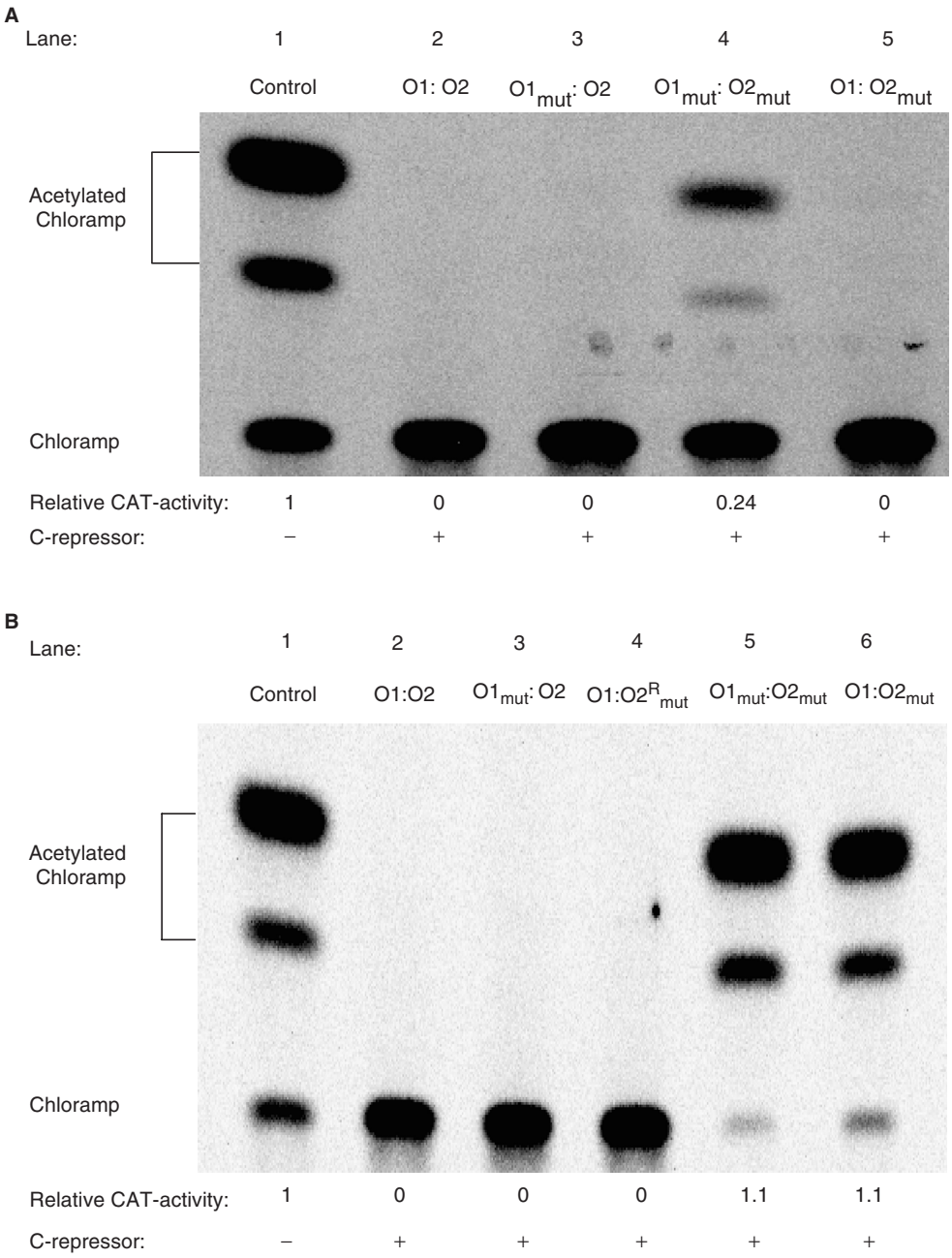

Figure 2. CAT assays showing the effects of the mutations in the direct repeats of P2 (**A**) and P2 Hy *dis* (**B**). In both cases, lane 1 is a control showing the strength of the Pe promoter in absence of the C repressor, and this CAT activity was set to 1. Lane 4 in B represents the operator where the O2 repeat extended with 2 nt corresponding to the O1 repeat. The relative CAT activity labeled 0, indicates that no activity could be detected in the phosphor imager analysis.

those generated in real time by SPR. To be able to analyze the association and dissociation by SPR we have used a Biacore 3000 system with streptavidine-coated SA chips containing four flow cells. The biotinylated 150-mers oligonucleotides were anchored to the surface of the SA chip at the respective cell. The first flow cell in all experiments contained non-specific DNA as a reference and a control in order to reduce background noise. DNA was recovered as the absolute resonance units (RU), i.e., the difference between the initial and final values of the bulk refractive index. The RU-values of the different DNA loaded flow cells are shown in Table 2.

Since the protein–DNA interactions may be affected by the flow rate, the initial kinetic studies were carried out at two flow rates, 2 and 30 µl/min, using a protein concentration of 23 pM. As can be see in Figure 5, differences in the binding responses of the C repressors to the surfaces containing the wild-type operators are observed. P2 C shows after injection an initially fast off rate, after which a very slow dissociation rate is reached. The response is ~200 U higher after the initial fast dissociation at 2 µl/min flow rate compared to the 30 µl/min flow rate (Figure 5A). P2 Hy *dis* C shows a triphasic dissociation, and it has only about a 50 RU higher

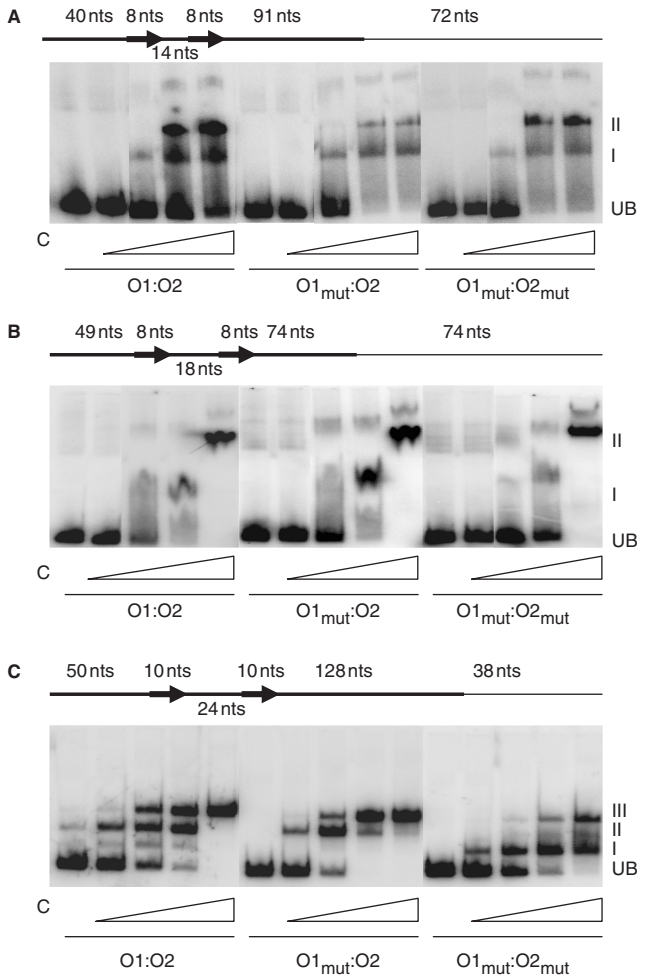

Figure 3. Binding of the C proteins to their cognate operators analyzed by electro mobility shifts. The line above the respective autoradiograph shows the labeled DNA fragment used. The bold line represents DNA originating from the phage, and the thin line originates from the vector. The arrows represent the operator half-sites. The numbers below the line indicate the distance between the half-sites. (**A**). P2 wild-type operator (lanes 1–5) operator with a point mutation in O1 (lanes 6–10) and with a point mutation in both O1 and O2 (lanes 11–15). The P2 C protein is added in increasing amounts as indicated (18.4–373 nM). (**B**) P2 Hy *dis* wild-type operator (lanes 1–5) operator with a point mutation in O1 (lanes 6–10) and with a point mutation in both O1 and O2 (lanes 11–15). The P2 Hy *dis* C protein is added in increasing amounts as indicated (0.2–52 nM). (**C**) Wϕ wild-type operator (lanes 1–5), operator with a point mutation in O1 (lanes 6–10) and with a point mutation in both O1 and O2 (lanes 11–15). The Wϕ C protein is added in increasing amounts as indicated (0.1–2.2 nM).

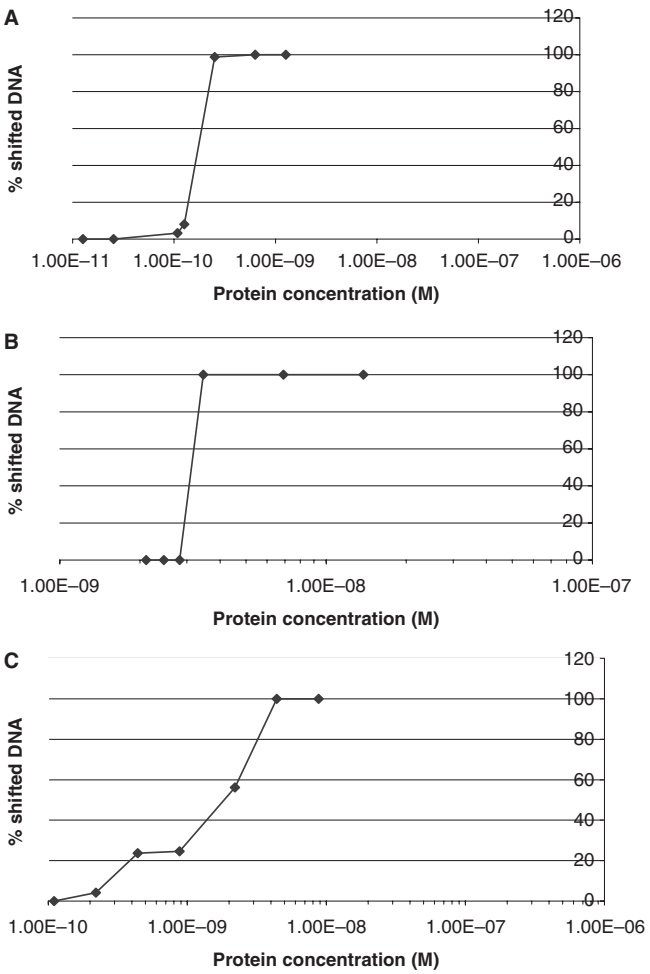

Figure 4. Titrations of complex formation between the C proteins and their respective wild-type operator, where the DNA concentration was constant and the protein concentration varied. The complex formation was determined using EMSA as the percent labeled DNA that was shifted out of total DNA loaded. (**A**) P2 C (0.03–1.3 nM). (**B**) P2 Hy *dis* C (2.1–13.8 nM). (**C**) Wϕ C (0.1–2.2 nM). Note that the protein concentration is in log scale and that only the P2 Hy *dis* C calculations are based on the experiment shown in Figure 3. The calculations are derived from titrations performed with the protein purifications having the highest specific activity.

response of C protein with a slow dissociation at 2 µl/min flow rate compared to the 30 µl/min (Figure 5B). The Wϕ C protein shows about a 200 RU higher response at 2 µl/min than at 30 µl/min (Figure 5C). Therefore, a 2 µl/min flow rate was used in our experiments. Saturation is not reached during the time span of the experiment for P2 C and Wϕ C, which might be due to a specific as well as an unspecific DNA binding of the C proteins to the DNA. The calculated ratio of bound C monomers/DNA molecule at the end of injection is about 3 for P2 C, 2 for P2 Hy *dis* C and 1.5 for Wϕ C.

To study the effects of the operator mutations, the SA chips were loaded with the wild-type operator (O1:O2), the operator containing one point mutation in one half-site (O1mut : O2), and the operator in which both half-sites were mutated (O1mut : O2mut). The RU-values are shown in Table 2. Since the P2 Hy *dis* O2 half-site already contains a natural point mutation (Figure 1) (4), a point mutation in only O1 (O1mut : O2) was used as a double mutant.

Determination of the kinetics of the interactions of the C repressor proteins and their wild type and mutated operators using the Biosensor system

The kinetic analyses were carried out with different protein concentrations. The first flow cell, containing non-specific DNA, was used as a negative control for the cells containing wild type or mutated operator sites.

Table 2. Amount of DNA template bound per flow cell

Flow cell[a]	DNA-template	RU[b]
Fc1	Random DNA	800
Fc2	O1:O2 (P2)	300
Fc3	O1mut: O2(P2)	260
Fc4	O1mut: O2mut(P2)	250
Fc1	Random DNA	440
Fc2	O1:O1(P2 Hy *dis*)	215
Fc3	O1mut: O2(P2 Hy *dis*)	210
Fc4	O1: O2mut(P2 Hy *dis*)	290
Fc1	Random DNA	557
Fc2	O1:O2 (Wϕ)	344
Fc3	O1mut: O2(Wϕ)	327
Fc4	O1mut: O2mut(Wϕ)	333

[a]One SA-chip per phage was used. In all three chips, the first flow cell (Fc1) was used as a reference. Other flow cells contained different operator constructions.
[b]The amount of bound DNA/cell is shown in RU.

The sensorgram data were analyzed with the BIA-evaluation software. The experimental data from each flow cell were used in the calculations unless otherwise stated, and evaluated for closeness of fit (chi-square) to the 1:1 Langmuir-binding model. The curves were normalized before the kinetic analysis, since there might be some conformational changes of DNA due to the binding of the C repressors. The calculations were carried out as described in Experimental Procedures.

P2 C. The relative responses (RU) of the binding of P2 C to its operator were found to correlate to the protein concentration (28.5–39.9 pM), i.e., the RU increased with increasing concentration. As can be seen in the sensogram (Figure 6A), the RU-values of the wild-type operator increase with 1200 RU during injection. However, the association rate of P2 C is biphasic, initially there is a very high-association rate that changes to a slower association rate, but it does not reach an equilibrium state at any concentration used. Estimations of the initial fast association rates (16–20 s) for the wild type and mutated operators indicate similar k_a. The range of the k_a varied between 2.3×10^6 and $1.5 \times 10^6\,M^{-1}s^{-1}$ (Table 3). The slow associaton rate constants calculated between 80 and 240 s, were between 6.5×10^5 and $3.9 \times 10^6\,M^{-1}s^{-1}$. The dissociation curve after the injection is also biphasic, i.e., after an initial fast dissociation of about half the RU, there is a steady state level with a very slow dissociation (Figure 6A). This may be interpreted in different ways. One possibility is that the initial fast dissociation rate is due to the release of non-specifically bound repressor, while the slow dissociation is the very tight complex of C with its operator. Alternatively, they represent two different forms of repressor–operator complexes where one represents a very tight binding. We believe the former is correct, and have calculated the dissociation rate constant from the steady state slow dissociation, i.e., between 260 and 510 s. The level of RU with a slow dissociation rate was reduced by 40 U at 23 pM between the wild-type operator and the O1mut : O2 operator, and the O1mut : O2mut operators showed to 20 U further

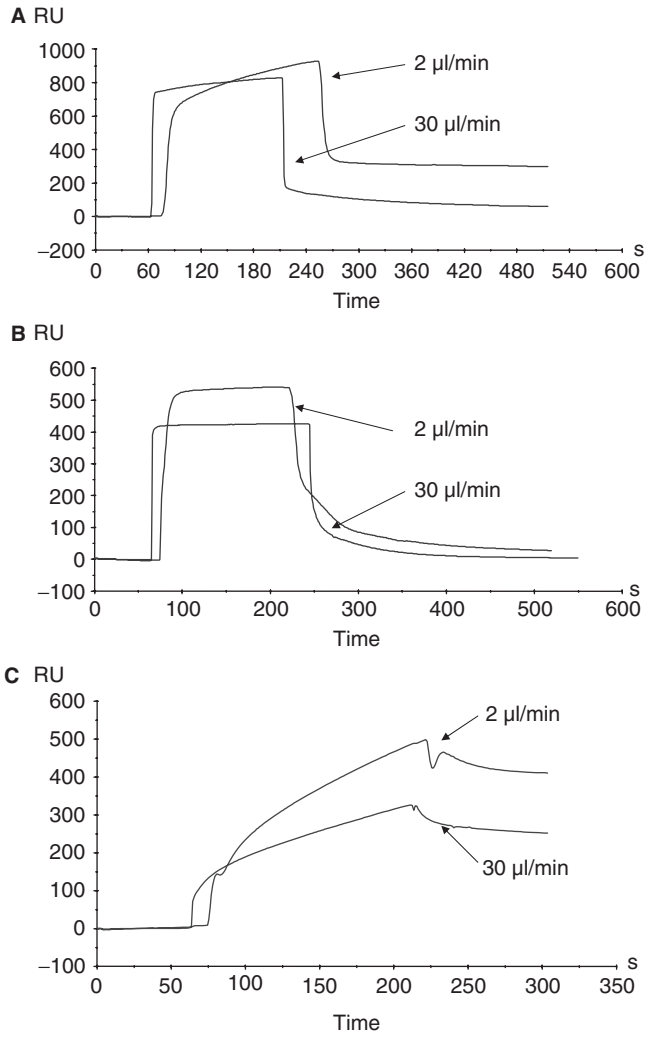

Figure 5. A comparison of the influence of the flow rate on the DNA binding of the C proteins to the respective wild-type operator in SPR analysis. (**A**) P2 C (**B**) P2 Hy *dis* C and (**C**). Wϕ C. The protein concentration was 23 pM. The injection time with Wϕ C at 30 µl/min was slightly longer compared with the injection time at 2 µl/min.

reduction. The dissociation rate constant k_d for the wild-type operator was $1.5 \times 10^{-3}\,s^{-1}$ and for the two mutated operators it was 1.8×10^{-3} and $2.1 \times 10^{-3}\,s^{-1}$ (Table 3).

These rate constants show that P2 C has a higher association rate and a lower dissociation rate to the wild-type operator and to the operator where O1 was mutated compared to the O1mut : O2mut operator. This means that P2 C forms a more stable complex with its wild-type operator and the O1mut : O2 operator than with the O1mut : O2mut operator. The calculated association constant K_A and the dissociation constant K_D were $1.5 \times 10^9\,M^{-1}$ and $6.3 \times 10^{-10}\,M$, respectively, for the wild-type operator compared to $2.2 \times 10^9\,M^{-1}$ and $4.7 \times 10^{-10}\,M$ for the O1mut : O2 operator and $7.0 \times 10^8\,M^{-1}$ and $1.4 \times 10^{-9}\,M$ for the O1mut:O2mut operator. These K_D and K_A-values confirm that P2 C has a stronger affinity and binding to the operators which also are functional *in vivo*.

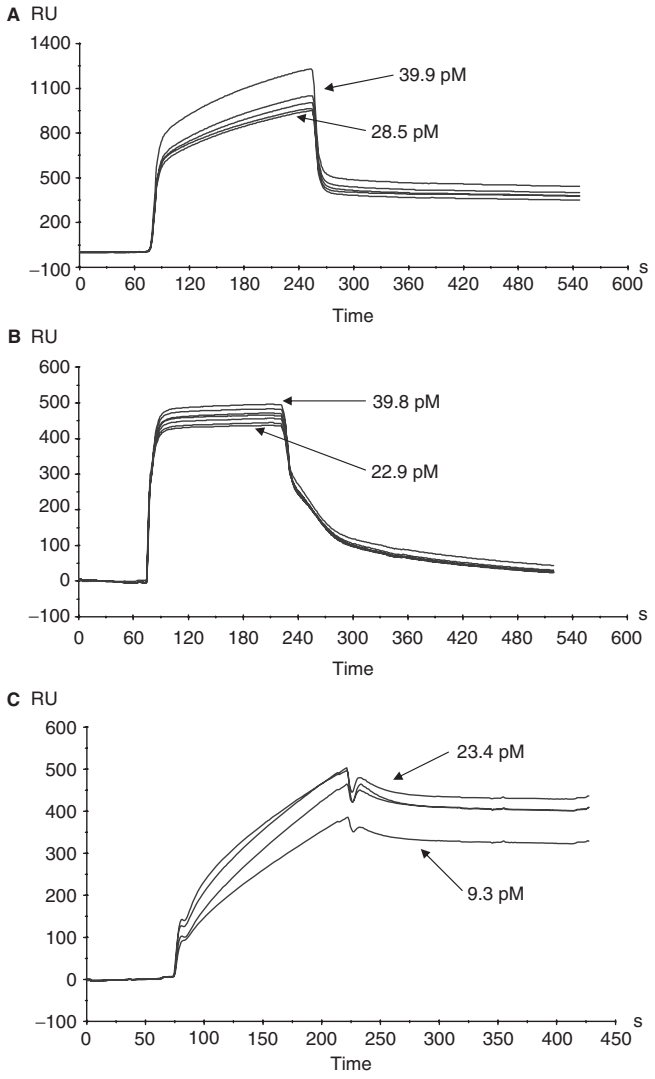

Figure 6. Sensorgrams showing the influence of protein concentration on the SPR signals using wild-type operators. (**A**) P2 C (**B**) P2 Hy *dis* C and (**C**) Wϕ C.

P2 Hy dis C. The sensorgrams using the P2 Hy *dis* C at different protein concentrations (22.9–39.8 pM) and the wild-type operator are shown in Figure 6B. The association rates as well as the dissociation rates seem to be triphasic at all concentrations. The values for the two fast association rates do not fit the 1:1 Langmuir model adapted for two binding sites, and the chi-square values are too high to give reliable rate constants. However, after ~120 s a very slow association rate is obtained, giving a k_a between 2.5 and $3.2 \times 10^5\,M^{-1}\,s^{-1}$ when measured between 80 and 210 s. Unlike P2 C, also the dissociation seems to be triphasic since after a fast dissociation event the sensograms indicate two different dissociation rates (Figure 6B). The dissociation rate constants for the wild type and the mutated operators are therefore calculated twice, between 240 and 300 s and between 300 and 510 s after injection, respectively. The first dissociation rate constants ($k_d{}^b$) were $4.9 \times 10^{-2}\,s^{-1}$ for the wild-type operator and 6.8×10^{-2} and $7.8 \times 10^{-2}\,s^{-1}$ for the mutated operators (Table 3). The second $k_d{}^c$ also shows a similar tendency for the operators, but a slightly increased dissociation rate constant was obtained for the operator containing a mutation in one half-site (Table 3). The level of RU with a slow dissociation rate at 23 pM was also slightly increased (5 U) between the wild type and the O1mut : O2 operator but the O1 : O2mut operator showed a 13 U reduction compared to the wild-type operator. The k_d-values obtained confirm that the dissociation is lower for the wild type and the O1 mutated operator, meaning that the complex formed with P2 Hy *dis* C and either the wild type or the O1mut : O2 operator is more stable than the complex with O1 : O2mut operator. An almost steady state was reached with all concentrations used as opposed to P2 and Wϕ C (see below) where the steady state could not be reached. This indicates that P2 Hy *dis* C has a lower level of non-specific binding compared to P2 and Wϕ C. This is also supported by the very fast binding seen in the EMSA analyses (Figure 4B), and by the fast association rate of P2 Hy *dis* C (Figure 6B). In spite of the steady state, neither the association constant K_A nor the dissociation constant K_D could be calculated because of some fluctuations between the concentrations after subtracting the reference from the analyte-binding sensograms. The lowest concentration, 22.9 pM had the highest RU. The RU increased from 25.7 to 28.8 pM, but decreased again from 28.8 to 39.8 pM (data not shown). It seems as if P2 Hy *dis* C could not bind efficiently to its operator at higher concentrations. Such a dose-dependent binding is not observed with P2 C.

Wϕ C. The sensorgrams obtained with Wϕ C at different protein concentrations (9.3–23.4 pM) with the wild-type operator are shown in Figure 6C. As for P2 C, the association of Wϕ C was biphasic and an equilibrium state was not reached at any protein concentration used. The initial very fast association rate constituted only ~20% of the RU obtained after 200 s. The estimated association rate constants determined between 17 and 20 s varied between 5.1×10^6 and $7.6 \times 10^6\,M^{-1}\,s^{-1}$. Also the dissociation was biphasic, but compared to P2 C, a much smaller fraction showed the very fast dissociation rate. The dissociation rate constant k_d was calculated between 275 and 400 s and varied between 1.5×10^{-4} and $7.7 \times 10^{-4}\,s^{-1}$ (Table 3). As for P2 C and P2 Hy *dis* C, Wϕ C has the highest affinity and the strongest binding to the wild-type operator. The O1mut : O2 operator has a slightly lower affinity and K_D-value than the wild-type operator, but a little higher compared with the O1mut : O2mut operator (Table 3). No difference in the level of RU of the complex with a slow dissociation rate was found between the wild type and operator mutants. Thus, Wϕ C, like P2 C and P2 Hy *dis* C, forms a stable protein–DNA complex with the operators that are active *in vivo*. This complex is, however, more stable than the complexes formed with P2 C and P2 Hy *dis* C to their respective operator, since a smaller fraction of the bound repressor shows a fast dissociation rate and the dissociation rate constant for the remaining complex is lower.

Table 3. The affinity and kinetic values[a] of the C proteins with their operators

Operator constructions of the phage	k_a ($M^{-1}s^{-1}$)	k_d[b] (s^{-1})	k_d[c] (s^{-1})	K_A (M^{-1})	K_D (M)
O1:O2 (P2)	2.3×10^6	1.5×10^{-3}		1.5×10^9	6.3×10^{-10}
O1mut: O2(P2)	3.9×10^6	1.8×10^{-3}		2.2×10^9	4.7×10^{-10}
O1mut: O2mut(P2)	1.5×10^6	2.1×10^{-3}		7.0×10^8	1.4×10^{-9}
O1:O2(P2 Hy *dis*)		4.9×10^{-2}	2.6×10^{-2}		
O1mut: O2(P2 Hy *dis*)		6.8×10^{-2}	2.3×10^{-2}		
O1mut:O2mut(P2 Hy *dis*)		7.8×10^{-2}	3.9×10^{-2}		
O1:O2(Wϕ)	7.6×10^6	7.7×10^{-4}		9.8×10^9	1.0×10^{-10}
O1mut: O2(Wϕ)	5.7×10^6	8.3×10^{-4}		7.4×10^9	1.3×10^{-10}
O1mut: O2mut(Wϕ)	5.1×10^6	8.8×10^{-4}		3.4×10^8	2.9×10^{-9}

[a]The values are the mean value obtained from the different protein concentrations.
[b]The values of P2 Hy *dis* C between the 240 and 300 s.
[c]The values of P2 Hy *dis* C between the 300 and 510 s.

DISCUSSION

In this work, the kinetics of the interactions between the small immunity repressors of three heteroimmune P2-like phages and their respective wild type and mutated operators are determined *in vitro* using purified proteins and compared to the capacities if the repressors to repress the early promoters *in vivo*. In spite of the homology between the repressors and similarities in the genetic switches that control the lytic growth versus the formation of lysogeny, our results show that the interactions of the immunity repressors with their operators differ extensively.

The transcriptional switches of the P2-like phages studied in this work all have face-to-face located promoters, as opposed to the lambdoid phages where the promoters are located back to back (14). The P2 promoters are controlled by two repressor proteins, C and Cox. In contrast to the transcriptional switch in phage lambda where the two repressors recognize the same operators although with different affinities, the P2 C and the Cox proteins recognize different operator sequences that overlap with the respective promoter they control. Furthermore, the P2 *C* gene seems to be expressed from the same promoter during establishment as well as during maintenance of the lysogenic state. This is in contrast to phage lambda, where the CII protein activates the P_{RE} promoter that is required for expression of CI during establishment of the lysogenic state, while promoter P_{RM} controls CI expression during the lysogenic state (14). In contrast to most temperate phages, the P2-like phages are not inducible by UV light, in accordance with the fact that the P2 C protein is not stimulated by RecA to undergo self-cleavage like lambda CI.

The transcriptional switch of the P2 related phage 186 has some features in common with P2, i.e., it has face to face located promoters, P_R and P_L, controlled by two repressors CI and Apl, where Apl has the equivalent functions of Cox (15), but the CI repressor has several features in common with lambda CI. It is about twice the size of P2 C and it recognizes inverted repeats (16). It can be expressed from two promoters, P_L and P_E, where the latter is activated by the CII protein (17). However, the N-terminus of the 186 CI protein contains an HTH motif that recognizes two types of inverted repeats (18), and like lambda CI the 186 CI protein act over large distances, since the repressors have additional binding sites at other locations and repressors bound at the different binding sites can interact forming different DNA loops depending on the CI concentration (19–21).

We have searched the genomes of P2 and Wϕ for possible alternative C binding sites, but no perfect matches to the directly repeated sequences were found. Several sites with 1 or 2 mismatches were found, but they are not located as two direct repeats so their involvement in possible long-range effects seems unlikely. It should, however, be kept in mind that the 186 CI repressor has the capacity to bind to two different sequences using the same DNA-binding domain (18).

In our electrophoretic mobility assays (EMSAs), the C proteins were shown to form different protein–DNA complexes, where the major complex formed with P2 Hy *dis* C has a slower migration compared to P2 C and Wϕ C. This slow migration might be caused by a different oligomeric state of P2 Hy *dis* C, or by a distortion of the DNA structure upon protein binding. The number of C proteins in the respective complex is not known, but the SPR analysis does not indicate a higher number of C proteins per DNA molecule for P2 Hy *dis* C. A genetic analysis of the P2 C and Wϕ C proteins has shown that in the absence of DNA they form dimers, but not higher oligomeric structures (8). During gel-filtration all C proteins elute at the same positions, indicating also that P2 Hy *dis* C is a dimer in solution (data not shown). Therefore, the higher mobility is more likely caused by a distortion of the DNA structure, possibly a consequence of the fact that the operator half-sites are separated by two and a half helical turns, and thus are not located on the same side of the DNA helix. A comparison of the complexes formed by P2 C and Wϕ C may indicate that they form similar complexes, but in the case of P2 there is no difference in the affinity to one half-site compared to the other. Using a circular permutation assay, the P2 and Wϕ C proteins have been shown to bend their respective DNA targets upon binding, and Wϕ C as opposed to P2 C is able to bind to only one half-site (8). This may explain why three retarded bands can be detected with Wϕ C but only two with P2 C.

Surprisingly, the EMSA failed to detect any significant differences in binding of the P2 C and P2 Hy *dis* C proteins to the operator mutants, not even to the operators having a point mutation on both half-sites. Using *in vivo* plasmid reporter gene systems, and the same point mutations no significant effect on the repression of the reporter gene is found with the single mutations, but a mutation in both half-sites showed a clear reduction in repression by P2 C and in P2 Hy *dis* and Wϕ repression is totally abolished (3, and this work). A possible explanation for this discrepancy between our *in vivo* and *in vitro* results is the configuration of the DNA targets. In the *in vivo* experiments the operator/promoter regions are in a supercoiled plasmid, but *in vitro* they are in the form of linear DNA fragments. Using SPR, however, point mutations in both half-sites clearly reduce the association constants and increases the dissociation constants of P2 and Wϕ C. Previous determinations of dissociation constants for P2 C has been obtained by filter-binding experiments where a constant concentration of P2 C was exposed to increasing concentrations of full length linear P2 DNA (22). The K_D obtained using a filter-binding assay with full-length P2 DNA covered the range 2.0×10^{-10} to 3.3×10^{-10} M, which is about the same as we found in our EMSA analysis (2.4×10^{-10} M) using a short DNA fragment containing O1 and O2. This implies that there are no additional strong binding sites for P2 C on the P2 genome. The dissociation constants measured by SPR have previously been shown to be lower compared to other methods, for example, using EMSA the lactose repressor-operator gives a K_D of 4.2×10^{-9} and using SPR the K_D was 2.0×10^{-10} (23). In this work, the K_D-values were found to be slightly higher using SPR in the case of P2 C and ~20-fold lower for Wϕ C.

The sensorgrams obtained in the SPR analysis for the P2 and P2 Hy *dis* C proteins show initially a very fast association rate, followed by a slower association rate. In the case of P2 Hy *dis* C the association seems triphasic and the two first cannot be fitted into the 1:1 Langmuir model, and therefore no association rate constants could be calculated and consequently no K_A or K_D could be determined. In the case of P2 C and Wϕ C, a biphasic association rate is seen in the sensogram and no saturation was obtained. Also the dissociation pattern differs between the C proteins. All show an initial very fast dissociation, but about half of the P2 C proteins show a very slow dissociation (k_d 1.5×10^{-3} s^{-1}), indicating two different protein–DNA complexes, which are also found in the case of Wϕ C where ~80% shows a very low dissociation (k_d 7.7×10^{-4} s^{-1}). In the case of P2 Hy *dis* C, the sensorgram indicates three different protein DNA complexes, 1/3 that dissociated very fast, another 1/3 that dissociates with a k_d of $\sim 5 \times 10^{-2}$ s^{-1}, while the remaining 1/3 has a k_d of 2.6×10^{-2} s^{-1}.

The above clearly indicates that evolution has driven the repressor–operator interactions into different directions that not only affect the sequence of the repressor proteins and their cognate operators, but also the kinetics of binding and dissociation and the type of complexes formed. A possible key to the different interactions of the C proteins with their respective operator revealed in this work might be the capacities of the C proteins to oligomerize upon binding to its DNA target. The CI protein of phage lambda is known to form dimers in solution, but octamers between dimers bound to different operator regions, with a looping of the DNA in between allowing long distant effects, are known (21). Furthermore, the crystal structure of phage 186 CI has revealed a heptamers of dimers around which the DNA is wrapped (24). The formation of higher oligomers upon DNA binding has also been shown for EthR, a repressor of the TetR/CamR family, which binds to its operator as an octamer, but in solutions it seems to be a monomer or dimers but not higher oligomers (25). This could be the case for the C proteins. A possible scenario is that in the absence of DNA the C proteins only forms dimers, but upon binding to their respective DNA targets they forms tetramers or higher oligomers. Possibly, the point mutations in both half-sites prevent tetramerization, but not binding of the dimeric form of the C protein to the mutated half-sites.

ACKNOWLEDGEMENTS

We thank Björn Lindqvist and Britt-Marie Sjöberg for helpful discussions, and Sara Renberg-Eriksson for providing plasmids. This work was supported by the Swedish Research Council. Funding to pay the Open Access publication charges for this article was provided by The Swedish Research Council.

Conflict of interest statement. None declared.

REFERENCES

1. Nilsson,A.S. and Haggård-Ljungquist,E. (2006). In Calendar,R (ed), *The bacteriophages, 2nd edn*. Oxford University Press, Oxford, pp. 365–390.
2. Ljungquist,E., Kockum,K. and Bertani,L.E. (1984) DNA sequence of the repressor gene and operator region of bacteriophage P2. *Proc. Natl Acad. Sci. USA*, **81**, 3988–3992.
3. Liu,T. and Haggård-Ljungquist,E. (1999) The transcriptional switch of bacteriophage Wϕ, a P2-related but heteroimmune coliphage. *J. Virol.*, **73**, 9816–9826.
4. Renberg-Eriksson,S.K., Ahlgren-Berg,A., DeGrooth,J. and Haggård-Ljungquist,E. (2001) Characterization of the developmental switch region of bacteriophage P2 Hy *dis*. *Virology*, **290**, 199–210.
5. Studier,F.W., Rosenberg,A.H., Dunn,J.J. and Dubendorff,J.W. (1990) Use of T7 RNA polymerase to direct expression of cloned genes. *Methods Enzymol.*, **185**, 60–89.
6. Liu,T., Renberg,S.K. and Haggård-Ljungquist,E. (1997) Derepression of prophage P2 by satellite phage P4: cloning of the P4 ε gene and identification of its product. *J. Virol.*, **71**, 4502–4508.
7. Liu,T., Renberg-Eriksson,S.K. and Haggård-Ljungquist,E. (1998) The E protein of satellite phage P4 acts as an anti-repressor by binding to the C protein of helper phage P2. *Mol. Microbiol.*, **30**, 1041–1050.
8. Ahlgren-Berg,A., Henriksson-Peltola,P., Sehlén,W. and Haggård-Ljungquist,E. (2007) A comparison of the DNA binding and bending capacities and the oligomeric states of the immunity repressors of heteroimmune coliphages P2 and Wϕ. Nucleic Acids Res., 35, XXX–XXX.
9. Brosius,J. (1984) Plasmid vectors for selection of promoters. *Gene*, **27**, 151–160.
10. Bradford,M.M. (1976) A rapid and sensitive method for the quantification of microgram quantities of protein utilizing the principle of protein-dye binding. *Anal. Biochem.*, **72**, 805–812.

11. Gorman,C.M., Moffat,L.F. and Howard,B.H. (1982) Recombinant genomes which express chloramphenicol acetyltransferase in mammalian cells. *Mol. Cell Biol.*, **2**, 1044–1051.
12. Renberg-Eriksson,S.K., Liu,T. and Haggård-Ljungquist,E. (2000) Interacting interfaces of the P4 antirepressor E and the P2 immunity repressor C. *Mol. Microbiol.*, **36**(5), 1148–1155.
13. Nilsson,M.T. and Widersten,M. (2004) Repertoire selection of variant single-chain Cro: toward directed DNA-binding specificity of helix-turn-helix proteins. *Biochemistry*, **43**, 12038–12047.
14. Ptashne,M. (1992) *A Genetic Switch: Phage λ And Higher Organisms, 2nd edn.* Cell Press & Blackwell Scientific Publications, Cambridge, MA.
15. Reed,M.R., Shearwin,F.E., Pell,L.M. and Egan,J.B. (1997) The dual role of Apl in prophage induction of coliphage 186. *Mol. Microbiol.*, **23**, 669–681.
16. Dodd,I.B. and Egan,J.B. (1996) DNA binding by the coliphage 186 repressor protein CI. *J. Biol. Chem.*, **271**, 11532–11540.
17. Neufing,P.J., Shearwin,K.E., Camerotto,J. and Egan,J.B. (1996) The CII protein of bacteriophage 186 establishes lysogeny by activating a promoter upstream of the lysogenic promoter. *Mol. Microbiol.*, **21**, 751–761.
18. Shearwin,K.E., Dodd,I.B. and Egan,J.B. (2002) The helix-turn-helix motif of the coliphage 186 immunity repressor binds to two distinct recognition sequences. *J. Biol. Chem.*, **277**, 3186–3194.
19. Dodd,I.B. and Egan,J.B. (2002) Action at a distance in CI repressor regulation of the bacteriophage 186 genetic switch. *Mol. Microbiol.*, **45**, 697–710.
20. Dodd,I.B., Perkins,A.J., Tsemitsidis,D. and Egan,J.B. (2001) Octamerization of lambda CI repressor is needed for effective repression of P(RM) and efficient switching from lysogeny. *Genes Dev.*, **15**, 3013–3022.
21. Dodd,I.B., Shearwin,K.E., Perkins,A.J., Burr,T., Hochschild,A. and Egan,J.B. (2004) Cooperativity in long-range gene regulation by the lambda CI repressor. *Genes Dev.*, **18**, 344–354.
22. Lundqvist,B. and Bertani,G. (1984) Immunity repressor of bacteriophage P2. Identification and DNA-binding activity. *J. Mol. Biol.*, **178**, 629–651.
23. Bondeson,K., Frostell-Karlsson,Å., Fägerstam,L. and Magnusson,G. (1993) Lactose repressor-operator DNA interactions: kinetic analysis by a surface plasmon resonance biosensor. *Anal. Biochem.*, **214**, 245–251.
24. Pinkett,H.W., Shearwin,K.E., Stayrook,S., Dodd,I.B., Burr,T., Hochschild,A., Egan,J.B. and Lewis,M. (2006) The structural basis of cooperative regulation at an alternate genetic switch. *Mol. Cell*, **21**, 605–615.
25. Engohang-Ndong,J., Baillat,D., Aumercier,M., Bellefontaine,F., Besra,G.S., Locht,C. and Baulard,A.R. (2004) EthR, a repressor of the TetR/CamR family implicated in ethionamide resistance in mycobacteria, octamerizes cooperatively on its operator. *Mol. Microbiol.*, **51**, 175–188.